Gold Catalysis

DOI: 10.1002/anie.201102487

Systematic Morphology Changes of Gold Nanoparticles Supported on CeO_2 during CO Oxidation**

*Tetsuya Uchiyama, Hideto Yoshida, Yasufumi Kuwauchi, Satoshi Ichikawa, Satoshi Shimada, Masatake Haruta, and Seiji Takeda**

Dedicated to the Fritz Haber Institute, Berlin, on the occasion of its 100th anniversary

Gold, the most stable metallic element, shows remarkable catalytic activity for CO oxidation even at room temperature.[1] Unlike platinum and palladium,[2] gold must be supported in the form of nanoparticles on crystalline metal oxides such as TiO_2[1] and CeO_2.[3] Despite extensive studies,[4–13] the mechanism of catalysis by gold nanoparticles (GNPs) is still unclear, in particular in relation to CO oxidation at room temperature. In the present study we observed a real Au/CeO_2 catalyst in CO/air mixtures by means of in situ environmental transmission electron microscopy (ETEM).[14–24] The catalyst was also characterized by catalytic chemical analyses. In real GNP catalysts, the structures of the GNPs are not identical at the atomic scale. Hence, we examined a large number of GNPs in the Au/CeO_2 catalyst using ETEM, and found that the majority of the GNPs behaved systematically, depending on the partial pressures of CO and O_2 at room temperature. GNPs remained faceted during CO oxidation in CO/air and became rounded, or fluctuating multifaceted with decrease of the partial pressure of CO relative to air. We also examined GNPs supported on a non-oxide crystal (TiC) with ETEM. In contrast to GNPs supported on CeO_2, switching the gases did not induce any morphology change of GNPs supported on TiC. These experimental results have provided a clue toward elucidation of the peculiar catalytic mechanism of supported GNPs. The interface between GNPs and CeO_2 support most likely plays an important role in the catalytic activity, especially the dissociation of O_2 molecules at room temperature. This work thus contributes to improving and developing real catalysts.

The Au/CeO_2 catalyst was prepared by the deposition precipitation method.[1] The conversion of CO to CO_2 reached 100% at room temperature, and the turnover frequency (TOF) of the catalyst was measured as $0.24\ mol_{CO}\,(mol_{Ausur})^{-1}\,s^{-1}$ at 303 K. The catalyst sample was examined in vacuum by conventional transmission electron microscopy before and after the oxidation of CO at atmospheric pressure and at 303 K for 5 h. As shown in Figure S1, it was confirmed that the average size and morphology of the GNPs remained unchanged after the oxidation of CO at atmospheric pressure. A detailed description of the catalyst is given in the Supporting Information.

First, we summarize the typical morphology of a GNP supported on CeO_2 in various environments at room temperature. During CO oxidation in 1 vol% CO/air gas mixture (1 vol% CO, 21 vol% O_2, 78 vol% N_2) at 1 mbar pressure, the GNP appeared to be faceted in the form of a stable polyhedron enclosed by the major {111} and {100} facets, as shown by Figure 1a. Unexpectedly, the GNP behaved differently, and became rounded in pure O_2 gas. The GNP exhibited major facets in both inactive N_2 gas at 1 mbar and in vacuum (Figure 1a). In N_2 gas, N_2 molecules collided with the surface of the GNP at a rate of $3\times10^6\ s^{-1}\,nm^{-2}$. By comparison of the GNP in N_2 gas and in vacuum (Figure 1a), we consider that the impacts of inactive N_2 molecules caused no significant

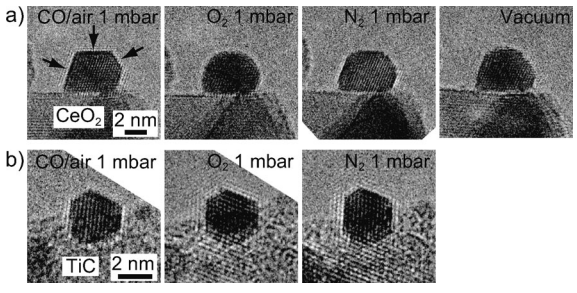

Figure 1. Typical morphology of a GNP in various environments. a) A GNP supported on CeO_2 during CO oxidation (1 vol% CO/air at 1 mbar), in pure O_2 gas (1 mbar), in pure N_2 gas (1 mbar), and in vacuum. b) A GNP supported on TiC during CO oxidation (1 vol% CO/air at 1 mbar), in pure O_2 gas (1 mbar), and in pure N_2 gas (1 mbar). The electron flux was estimated to be $4\ A\,cm^{-2}$.

[*] T. Uchiyama, Y. Kuwauchi
Graduate School of Science, Osaka University
1-1 Machikaneyama, Toyonaka, Osaka 560-0043 (Japan)
Dr. H. Yoshida, Prof. S. Takeda
The Institute of Scientific and Industrial Research, Osaka University
8-1 Mihogaoka, Ibaraki, Osaka 567-0047 (Japan)
E-mail: takeda@sanken.osaka-u.ac.jp
Dr. S. Ichikawa
Institute for Nanoscience Design, Osaka University
1-3 Machikaneyama, Toyonaka, Osaka 560-8531 (Japan)
S. Shimada, Prof. M. Haruta
Graduate School of Urban Environmental Sciences
Tokyo Metropolitan University
1-1 Minami-osawa, Hachioji, Tokyo 192-0397 (Japan)

[**] This study was supported by a Grant-in-Aid for Specially Promoted Research, Grant No. 19001005 from the Ministry of Education, Culture, Sports, Science and Technology (Japan). The authors also thank T. Akita, S. Tanaka, K. Tanaka, and M. Kohyama of AIST for their interest in this study, and R. Matsumoto, Y. Kohigashi, and K. Matsuura for their support with ETEM experiments.

Supporting information for this article is available on the WWW under http://dx.doi.org/10.1002/anie.201102487.

© 2011 Wiley-VCH Verlag GmbH & Co. KGaA, Weinheim

effect on the GNP surface. A similar change in morphology of other GNPs in vacuum, air at 3.4 mbar, and 1 vol% CO/air at 3.4 mbar is shown in Figure S2 in both cross-sectional view (Figure S2a) and plan view (Figure S2b). The GNP morphology change was found to be reversible between the different gases and in vacuum (Figure S3).

GNPs supported on crystalline TiC remained polyhedral in all of the gas environments including pure O_2 gas, as shown in Figure 1b, and high catalytic activity of Au/TiC has never been reported.[25] Hence, the morphology change of GNPs in the Au/CeO_2 catalyst is associated with the catalytic activity of that catalyst.

We pursued the morphology change of GNPs in the Au/CeO_2 catalyst by systematically changing the partial pressures of CO and O_2 gases. The morphology of the GNPs in the presence of gas mixtures was characterized numerically by the relative morphology index, M (Supporting Information), that we introduced to determine quantitatively whether the morphology was faceted or rounded. We determined the morphology of several (five to 15) GNPs in a given gas. When more than 70% of the GNPs were classified with the same morphology, we concluded that the morphology of the GNPs in that gas environment was statistically determined. When the morphology of GNPs in a gas was disperse, or the percentage of the GNPs belonging to the major morphology was smaller than 70%, we concluded that the morphology was statistically mixed. In this way we established a morphology diagram for the Au/CeO_2 catalyst (Figure 2) that represents the dependence of the morphology of the GNPs on the partial pressures of CO (P(CO)) and O_2 (P(O_2)). To our knowledge, these systematic microstructural data for an operating GNP catalyst were obtained for the first time. The morphology diagram in Figure 2 shows that faceted GNPs were stable at higher CO partial pressures; with decrease of the partial pressure of CO, the faceted GNPs became rounded. When the partial pressure of O_2 was sufficiently low, GNPs partly returned to the faceted form, even at low CO partial pressures.

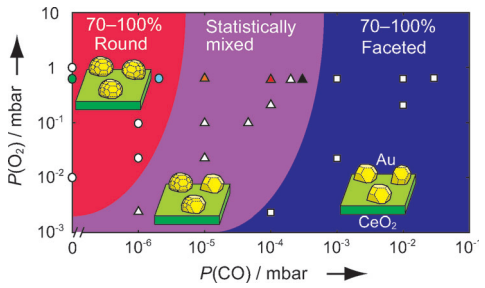

Figure 2. Morphology of GNPs supported on CeO_2, as a function of the partial pressures of CO (P(CO)) and O_2 (P(O_2)) in CO/air gaseous mixtures. The squares, triangles and circles represent faceted, statistically mixed, and rounded (dynamic multi-faceted) morphologies, respectively. Black, red, orange triangles, light blue and green circles represent the observation conditions in Figure 3b, c, d, e, and f, respectively. A morphology diagram as a function of the total pressure of the gases (CO and O_2), P(CO) + P(O_2) and the ratio of partial pressures, P(CO)/P(O_2), or reducing potential is also given in Figure S4 to simplify the physical meanings of the diagram.

Figure 3 shows in situ observations of the change in morphology of a GNP on decreasing the partial pressure of

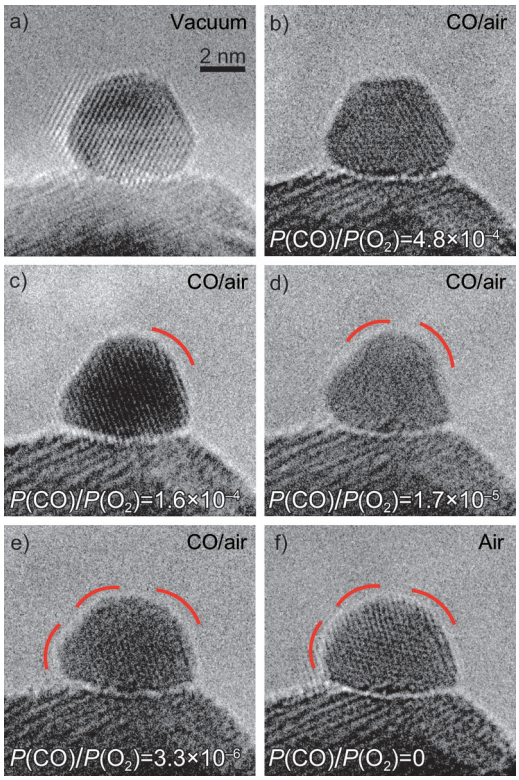

Figure 3. Morphology change of a GNP with decrease of the partial pressure of CO in CO/air mixtures with total pressure 3 mbar. a) Vacuum (reference); b) 3×10^{-4} mbar CO; c) 1×10^{-4} mbar CO; d) 1×10^{-5} mbar CO; e) 2×10^{-6} mbar CO; f) 0 mbar CO (air). The ratio of partial pressures of CO to O_2 (P(CO)/P(O_2)) is shown in each image. The electron flux was estimated to be 4.7 A cm^{-2}.

CO at constant total pressure (3 mbar) of CO/air mixtures. The GNP was faceted in 0.01 vol% CO/air ($P(CO) = 3\times10^{-4}$ mbar, $P(O_2) = 6.3\times10^{-1}$ mbar; Figure 3b). It should be noted that the partial pressure of O_2 was three orders of magnitude higher than that of CO. On decreasing the partial pressure of the minor CO gas, the GNP became partly rounded (Figure 3c–e). On completely removing CO, the GNP appeared to be fully rounded (Figure 3f). Clearly, this in situ observation proves that CO molecules stabilize the major {111} and {100} facets of GNPs. Theoretical analyses[12,26,27] suggest that CO molecules are adsorbed on the surface of GNPs, that is, on terraces and/or edges, during CO oxidation. According to Molina and Hammer,[26] faceted GNPs become stable when the terraces and edges are covered by CO molecules rather than other kinds of molecules such as O_2, O, and N_2. In the situation shown in Figure 3b (0.01 vol% CO), we estimate that the collision rate of CO molecules with the surface of the GNP was 10^3 s^{-1} nm^{-2}. Though a considerable number of adsorbed CO molecules may be expelled by electron irradiation as discussed later, we conclude that predominantly CO molecules populate the surface of the

 © 2011 Wiley-VCH Verlag GmbH & Co. KGaA, Weinheim

GNPs. Thus both experimental and theoretical studies[26] have now shown that adsorption of CO molecules stabilizes the faceted GNPs.

The rounded GNP morphology in O_2 gas (Figure 1a) and air (Figure 3f, Figure S2) originates from fluctuating multifaceted surfaces. Examination of each frame in in situ ETEM observation showed that the minority {110} facet emerged frequently in addition to the major {111} and {100} facets (Figure 4b), while in CO-rich gas, the major facets were much

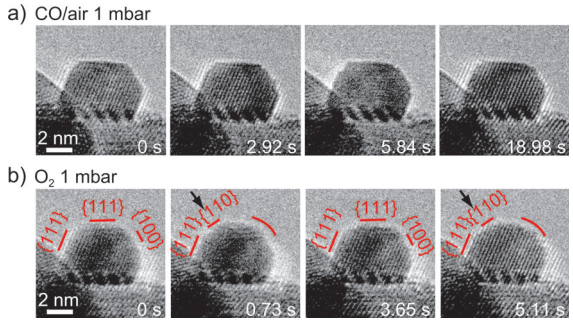

Figure 4. Frames from in situ ETEM observations of a GNP, during CO oxidation in a) 1 vol% CO/air (1 mbar), and b) O_2 (1 mbar). In O_2 gas, the GNP exhibited {111}, {100}, and {110} facets dynamically, while in CO/air the major {111} and {100} facets were stable. The electron flux was estimated to be 4.6 $A\,cm^{-2}$.

more stable (Figure 4a). In movies S1–S4, frames that exhibit the fluctuating multifaceted morphology in O_2 gas and the stable major facets in other gases and in vacuum can be seen. Because of the fluctuation between {111}, {100}, and {110} facets with time, GNP appears to be rounded. A theoretical study suggested that once oxygen atoms are formed, they can be adsorbed on both flat and defective surfaces of a free-standing GNP.[12,13] More interestingly, recent ab initio computations[28] showed that oxygen atoms can be adsorbed on not only the major {111} and {100} facets but also the minority {110} facet of GNPs. These results best correspond to the rounded morphology in O_2 gas (Figure 4b). Given that GNPs in Au/TiC never appear by ETEM observation to be rounded in O_2 gas (Figure 1b), the rounded morphology in Au/CeO_2 can be correlated with the catalytic activity. Oxygen atoms from dissociation of O_2 molecules by the Au/CeO_2 catalyst cause the rounded morphology, though it is likely that the dissociation process is promoted partially by electron irradiation. During CO oxidation in the CO/air mixture, CO molecules on the surface of GNPs are oxidized by the oxygen atoms at room temperature. The dissociation sites of oxygen molecules may not be on the surface of GNPs; they are more likely to be at the perimeter interface between GNPs and CeO_2 support and/or the surface of the CeO_2 support. It is noteworthy that residual gases, including moisture, inevitably exist even "in vacuum" in ETEM, as described in the Experimental Section. It is also possible, therefore, that active oxygen-related species rather than oxygen atoms may be formed in the ETEM environment.[29]

The environments around catalysts in ETEM are different from those in usual catalytic reactions because of electron irradiation and the relatively low pressures of gases. Nevertheless, we conclude that the catalytic reactions were occurring during the ETEM observations. This conclusion is based on estimates of the rates of oxidation, adsorption, and desorption of CO molecules on the GNPs. Firstly, the rate of CO oxidation per surface Au atom of the real catalyst was experimentally estimated as 0.24 s^{-1} (TOF) by means of catalytic activity measurements in CO 1 vol%/air at room temperature (see the Supporting Information). Secondly, the maximum possible adsorption rate of CO molecules per surface Au atom was estimated to be $7\times10^{2}\,s^{-1}$ in the environment (CO 1 vol%/air at 1 mbar at room temperature). This rate was obtained as the product of the collision rate of CO molecules per surface Au atom ($1.8\times10^{3}\,s^{-1}$) and the initial adsorption probability (0.40).[30] Thirdly, the desorption of CO molecules from the surface of the GNPs is caused by electron irradiation. Thermal desorption is probably enhanced because of a temperature rise in the GNPs under electron irradiation. The increase in temperature of the GNPs by electron irradiation under our experimental conditions was roughly estimated to be about 40 K (see the Supporting Information). According to literature,[31,32] the thermal desorption rate of CO from the surface of GNPs at 340 K was estimated to be $3.4\times10^{-2}\,s^{-1}$.[32] As a reference, the thermal desorption rate at higher temperatures such as 360 and 380 K was also estimated to be $1.4\times10^{-1}\,s^{-1}$ and $5.1\times10^{-1}\,s^{-1}$, respectively. Therefore, even considering the electron-irradiation enhanced thermal desorption, we conclude that CO remained adsorbed in our experiment. More precisely, the thermal desorption rate of CO depends on the adsorption sites on the surface of the GNPs through the adsorption/desorption energy and the vibration frequency of CO molecules.[26,27,33–35] The adsorption sites were not identified in our experiment although it has been suggested that CO molecules are mostly adsorbed at preferential adsorption sites such as at edges and corners.[26,27,36,37] In addition, electron irradiation probably leads to electron-stimulated desorption and knock-on sputtering (see the Supporting Information). Considering all the possible desorption processes, the total desorption rate is estimated to be about $10^{-1}\,s^{-1}$ (see the Supporting Information). Hence, the maximum possible adsorption rate of CO molecules ($7\times10^{2}\,s^{-1}$) is much higher than the total rate of desorption ($10^{-1}\,s^{-1}$) and consumption by oxidation, that is, TOF (0.24 s^{-1}). Consequently, adsorbed CO molecules continue to cover the surface of GNPs, thereby stabilizing the major {111} and {100} facets (Figure 4a). It is interesting to note that atomic steps rarely appear on the surface of GNPs even in vacuum. These random events are simply attributed to the knock damage of gold atoms on the surface (Figure 4 and Movies S1–S4). As mentioned earlier, electron irradiation may partially promote dissociation of oxygen molecules. Finally, the GNPs exhibit the same morphology in vacuum after exposure to environments at different gas pressures (Figure S1 and S3). Therefore, the observations obtained under relatively low gas pressures in this study are useful to understand the morphology of active GNPs under realistic catalytic conditions.

In summary, we have systematically studied Au/CeO_2 catalysts using ETEM. By establishing the morphology diagram and considering electron irradiation effects, we

 © 2011 Wiley-VCH Verlag GmbH & Co. KGaA, Weinheim

conclude that the morphology change correlates well with the catalytic activity of supported GNPs on CeO_2. During CO oxidation in CO/air mixtures, 1) CO molecules are adsorbed on the surface of GNPs, and stabilize GNPs with polyhedral shape enclosed by the major {111} and {100} facets, and 2) O_2 molecules are dissociated into oxygen atoms or active oxygen-related species by the catalysts, partly with the aid of electron irradiation, thus inducing the formation of rounded or fluctuating multifaceted surfaces of GNPs. CO molecules accordingly oxidize at room temperature. It is probable that O_2 molecules are preferentially dissociated at the perimeter interface between GNPs and the CeO_2 support and/or the surface of the CeO_2 support.

Experimental Section

Au/CeO_2 catalyst samples were supported on a carbon-coated microgrid backed by a Cu mesh 3 mm in diameter. A mesh with samples was fixed on a specimen holder and transferred to an ETEM (FEI Tecnai F20 equipped with an environmental cell)[22,23] operated at 200 kV. The samples were observed in various gases in sequence; the time required to switch gases in the ETEM was 1200–1800 s. The morphology of GNPs in a gas did not depend on the sequence of gases. The nominal impurity levels of all gases were less than 0.0005 vol%. Residual gas in the ETEM was measured with a quadrupole mass spectrometer. The total pressure of residual gas was about 6.5×10^{-4} mbar, of which the partial pressures of constituent gases were H_2O: 5.9×10^{-4} mbar, N_2: 0.3×10^{-4} mbar, O_2: 0.2×10^{-4} mbar, and CO_2: 0.1×10^{-4} mbar. Using a CCD camera, ETEM images of 512×512 pixels were recorded at 1 frame per 0.65 or 0.73 s. CeO_2 supports are known to be much more stable under electron irradiation than other metal oxide supports such as TiO_2.[38] To minimize electron-irradiation damage, samples were irradiated with electron fluxes smaller than 5.3 A cm^{-2} (3.3×10^5 electrons s^{-1} nm^{-2}) only for observing and recording ETEM images. Electron energy loss spectroscopy revealed no detectable changes in the oxygen K edge and Ce M edge of CeO_2 supports after ETEM observation in vacuum, thus indicating that loss of oxygen in CeO_2 supports induced by electron irradiation was negligibly small or possibly recovered from the residual oxygen in the ETEM.

Received: April 11, 2011
Revised: August 25, 2011
Published online: September 9, 2011

Keywords: CeO_2 · CO oxidation · environmental TEM · gold · heterogeneous catalysis

[1] M. Haruta, *Catal. Today* **1997**, *36*, 153 – 166.
[2] R. Imbihl, G. Ertl, *Chem. Rev.* **1995**, *95*, 697 – 733.
[3] S. D. Gardner, G. B. Hoflund, D. R. Schryer, J. Schryer, B. T. Upchurch, E. J. Kielin, *Langmuir* **1991**, *7*, 2135 – 2139.
[4] M. Haruta, N. Yamada, T. Kobayashi, S. Iijima, *J. Catal.* **1989**, *115*, 301 – 309.
[5] M. Haruta, *Chem. Rec.* **2003**, *3*, 75 – 87.
[6] M. Haruta, *CATTECH* **2002**, *6*, 102 – 115.
[7] G. C. Bond, D. T. Thompson, *Gold Bull.* **2000**, *33*, 41 – 51.
[8] M. S. Chen, D. W. Goodman, *Science* **2004**, *306*, 252 – 255.
[9] M. S. Chen, D. W. Goodman, *Acc. Chem. Res.* **2006**, *39*, 739 – 746.
[10] Q. Fu, H. Saltsburg, M. Flytzani-Stephanopoulos, *Science* **2003**, *301*, 935 – 938.
[11] W. Deng, J. De Jesus, H. Saltsburg, M. Flytzani-Stephanopoulos, *Appl. Catal. A* **2005**, *291*, 126 – 135.
[12] M. Mavrikakis, P. Stoltze, J. K. Nørskov, *Catal. Lett.* **2000**, *64*, 101 – 106.
[13] Y. Xu, M. Mavrikakis, *J. Phys. Chem. B* **2003**, *107*, 9298 – 9307.
[14] E. D. Boyes, P. L. Gai, *Ultramicroscopy* **1997**, *67*, 219 – 232.
[15] T. W. Hansen, J. B. Wanger, P. L. Hansen, S. Dahl, H. Topsøe, C. J. H. Jacobsen, *Science* **2001**, *294*, 1508 – 1510.
[16] S. Helveg, C. López-Cartes, J. Sehested, P. L. Hansen, B. S. Clausen, J. R. Rostrup-Nielsen, F. Abild-Pedersen, J. K. Nørskov, *Nature* **2004**, *427*, 426 – 429.
[17] R. Sharma, Z. Iqbal, *Appl. Phys. Lett.* **2004**, *84*, 990 – 992.
[18] P. L. Gai, E. D. Boyes, J. C. Bart, *Philos. Mag. A* **1982**, *45*, 531 – 547.
[19] P. L. Gai, B. C. Smith, G. Owen, *Nature* **1990**, *348*, 430 – 432.
[20] P. L. Gai, K. Kourtakis, E. D. Boyes, *Catal. Lett.* **2005**, *102*, 1 – 7.
[21] S. Giorgio, M. Cabié, C. R. Henry, *Gold Bull.* **2008**, *41*, 167 – 173.
[22] H. Yoshida, S. Takeda, T. Uchiyama, H. Kohno, Y. Homma, *Nano Lett.* **2008**, *8*, 2082 – 2086.
[23] H. Yoshida, T. Shimizu, T. Uchiyama, H. Kohno, Y. Homma, S. Takeda, *Nano Lett.* **2009**, *9*, 3810 – 3815.
[24] H. Yoshida, S. Takeda, *Phys. Rev. B* **2005**, *72*, 195428.
[25] L. K. Ono, D. Sudfeld, B. R. Cuenya, *Surf. Sci.* **2006**, *600*, 5041 – 5050.
[26] L. M. Molina, B. Hammer, *Phys. Rev. B* **2004**, *69*, 155424.
[27] L. M. Molina, B. Hammer, *Appl. Catal. A* **2005**, *291*, 21 – 31.
[28] H. Shi, C. Stampfl, *Phys. Rev. B* **2008**, *77*, 094127.
[29] M. Daté, M. Okumura, S. Tsubota, M. Haruta, *Angew. Chem.* **2004**, *116*, 2181 – 2184; *Angew. Chem. Int. Ed.* **2004**, *43*, 2129 – 2132.
[30] E. Kadossov, J. Justin, M. Lu, D. Rosenmann, L. E. Ocola, S. Cabrini, U. Burghaus, *Chem. Phys. Lett.* **2009**, *483*, 250 – 253.
[31] J. C. Clark, S. Dai, S. H. Overbury, *Catal. Today* **2007**, *126*, 135 – 142.
[32] A. Pitois, A. Pilenga, A. Pfrang, G. Tsotridis, *Int. J. Hydrogen Energy* **2011**, *36*, 4375 – 4385.
[33] M. Gajdoš, A. Eichler, J. Hafner, *J. Phys. Condens. Matter* **2004**, *16*, 1141 – 1164.
[34] A. Hussain, D. C. Ferré, J. Gracia, B. E. Nieuwenhuys, J. W. Niemantsverdriet, *Surf. Sci.* **2009**, *603*, 2734 – 2741.
[35] F. Mehmood, A. Kara, T. S. Rahman, C. R. Henry, *Phys. Rev. B* **2009**, *79*, 075422.
[36] I. Nakamura, A. Takahashi, T. Fujitani, *Catal. Lett.* **2009**, *129*, 400 – 403.
[37] S. Derrouiche, P. Gravejat, D. Bianchi, *J. Am. Chem. Soc.* **2004**, *126*, 13010 – 13015.
[38] M. I. Buckett, J. Strane, D. E. Luzzi, J. P. Zhang, B. W. Wessels, L. D. Marks, *Ultramicroscopy* **1989**, *29*, 217 – 227.

 © 2011 Wiley-VCH Verlag GmbH & Co. KGaA, Weinheim